

Observation of an enhancement in $e^+e^- \rightarrow \Upsilon(1S)\pi^+\pi^-$, $\Upsilon(2S)\pi^+\pi^-$, and $\Upsilon(3S)\pi^+\pi^-$ production at Belle

K.-F. Chen (for the Belle collaboration)

Department of Physics, National Taiwan University, Taipei

We measure the production cross sections for $e^+e^- \rightarrow \Upsilon(1S)\pi^+\pi^-$, $\Upsilon(2S)\pi^+\pi^-$, and $\Upsilon(3S)\pi^+\pi^-$ as a function of \sqrt{s} , for \sqrt{s} between 10.83 GeV and 11.02 GeV. The data consists of 7.9 fb⁻¹ collected with the Belle detector at the KEKB e^+e^- collider. We observe an enhancement in the production of these final states that is not well-described by the conventional $\Upsilon(10860)$ lineshape. A fit using a single Breit-Wigner resonance shape yields a peak mass of $10889.6 \pm 1.8(\text{stat}) \pm 1.5(\text{syst})$ MeV/ c^2 and a width of $54.7_{-7.2}^{+8.5}(\text{stat}) \pm 2.5(\text{syst})$ MeV/ c^2 .

1. INTRODUCTION

Recently a large number of charmonium-like meson states have been discovered. Some of these states have been identified as expected charmonium resonances. More interestingly, other resonances, such as the $X(3872)$ [1] and $Y(4260)$ [2], which decay through a dipion transition into $J/\psi\pi^+\pi^-$, do not seem to fit into the conventional $c\bar{c}$ spectrum. Possible interpretations for these exotic states include the multiquark states, mesonic-molecules ($c\bar{q}-\bar{c}q$, where c is a charm quark and q represents a u -, d - or s -quark), or $c\bar{c}g$ “hybrids” (where g is a gluon).

The state $Y(4260)$ is a broad $J^{PC} = 1^{--}$ resonance and has been confirmed by CLEO [3] with a dedicated scan of $J/\psi\pi^+\pi^-$ yield as a function of center-of-mass (CM) energy. It has an unexpectedly large $J/\psi\pi^+\pi^-$ partial width [2, 3]. A second enhancement just below the peak of $Y(4260)$ has been reported by Belle [4]. An independent enhancement seen in the $\psi'\pi^+\pi^-$ mass spectrum with a mass peak around 4.32–4.36 GeV/ c^2 [5, 6] does not agree with the measured $Y(4260)$ mass, and brings new challenges regarding the proper interpretation of the quark content for the new states.

Recent studies of the bottomonium system shed light on the structure of these charmonium-like resonances but also present new puzzles. Using a data sample recorded by the Belle detector at a single center-of-mass energy near the peak of the $\Upsilon(10860)$ resonance, anomalously large $\Upsilon(1S)\pi^+\pi^-$ and $\Upsilon(2S)\pi^+\pi^-$ production rates have been observed [7]. If these signals are attributed entirely to dipion transitions from the $\Upsilon(10860)$ resonance, the corresponding partial widths are more than two orders of magnitude larger than those from corresponding transitions from the lower $\Upsilon(2S)$, $\Upsilon(3S)$, and $\Upsilon(4S)$ states. A possible explanation is a bottomonium counterpart to the $Y(4260)$, denoted Y_b [8], which may overlap with the nominal $b\bar{b}$ radial excitation $\Upsilon(5S)$. Alternative explanations include a new nonperturbative approach [9] for the calculation of the decay widths of dipion transitions of heavy quarkonia, the presence of final state interactions [10], or the existence of an intermediate state [11]. These hypotheses can be distinguished by a measurement of the energy dependence of the cross sections for $e^+e^- \rightarrow \Upsilon(nS)\pi^+\pi^-$ ($n = 1, 2, 3$) within the $\Upsilon(10860)$ energy region.

2. THE ANALYSIS

Here we report the observation of an enhancement in the production of $\Upsilon(1S)\pi^+\pi^-$, $\Upsilon(2S)\pi^+\pi^-$, and $\Upsilon(3S)\pi^+\pi^-$ via e^+e^- annihilation, using data samples collected in a dedicated energy scan at CM energies $\sqrt{s} \simeq 10.83, 10.88, 10.90, 10.93, 10.96, \text{ and } 11.02$ GeV with the Belle detector at the KEKB e^+e^- energy-asymmetric collider [12].

The Belle detector is a large-solid-angle magnetic spectrometer that consists of a silicon vertex detector (SVD), a central drift chamber (CDC), an array of aerogel threshold Cherenkov counters (ACC), a barrel-like arrangement of time-of-flight scintillation counters (TOF), and an electromagnetic calorimeter (ECL) comprised of CsI(Tl) crystals located inside a superconducting solenoid that provides a 1.5 T magnetic field. An iron flux-return located outside

Table I: Center-of-mass energy (\sqrt{s}), integrated luminosity (\mathcal{L}), signal yield (N_s), reconstruction efficiency, and observed cross section (σ) for $e^+e^- \rightarrow \Upsilon(1S)\pi^+\pi^-$, $\Upsilon(2S)\pi^+\pi^-$, and $\Upsilon(3S)\pi^+\pi^-$. The first uncertainty is statistical, and the second is systematic.

\sqrt{s} (GeV)	\mathcal{L} (fb ⁻¹)	$e^+e^- \rightarrow \Upsilon(1S)\pi^+\pi^-$			$e^+e^- \rightarrow \Upsilon(2S)\pi^+\pi^-$			$e^+e^- \rightarrow \Upsilon(3S)\pi^+\pi^-$		
		N_s	Eff.(%)	σ (pb)	N_s	Eff.(%)	σ (pb)	N_s	Eff.(%)	σ (pb)
10.8275	1.68	$10.6_{-3.3}^{+4.0}$	43.8	$0.58_{-0.18}^{+0.22} \pm 0.06$	$24.0_{-4.9}^{+5.6}$	34.9	$2.11_{-0.43}^{+0.49} \pm 0.25$	$1.8_{-1.1}^{+1.8}$	20.5	$0.24_{-0.15}^{+0.24} \pm 0.03$
10.8825	1.83	$43.4_{-6.5}^{+7.2}$	43.1	$2.22_{-0.33}^{+0.37} \pm 0.16$	$68.8_{-8.3}^{+9.0}$	35.4	$5.49_{-0.66}^{+0.72} \pm 0.62$	$14.9_{-3.7}^{+4.3}$	24.5	$1.52_{-0.38}^{+0.44} \pm 0.19$
10.8975	1.41	$26.2_{-5.1}^{+5.8}$	43.2	$1.74_{-0.34}^{+0.39} \pm 0.14$	$45.4_{-6.7}^{+7.4}$	35.6	$4.69_{-0.69}^{+0.77} \pm 0.53$	$10.3_{-3.1}^{+3.7}$	25.7	$1.31_{-0.39}^{+0.47} \pm 0.16$
10.9275	1.14	$11.1_{-3.3}^{+4.0}$	42.6	$0.92_{-0.27}^{+0.33} \pm 0.08$	$9.7_{-3.1}^{+3.8}$	35.9	$1.23_{-0.39}^{+0.48} \pm 0.17$	$2.9_{-1.5}^{+2.2}$	27.5	$0.42_{-0.22}^{+0.32} \pm 0.05$
10.9575	1.01	$3.9_{-1.9}^{+2.6}$	42.5	$0.37_{-0.18}^{+0.24} \pm 0.04$	$2.0_{-1.3}^{+2.0}$	36.4	$0.28_{-0.18}^{+0.28} \pm 0.05$	$-1.8_{-3.0}^{+2.5}$	29.4	$-0.28_{-0.47}^{+0.39} \pm 0.03$
11.0175	0.86	$4.9_{-2.1}^{+2.8}$	42.0	$0.55_{-0.24}^{+0.31} \pm 0.05$	$5.5_{-2.4}^{+3.1}$	36.0	$0.92_{-0.40}^{+0.52} \pm 0.17$	$4.3_{-1.9}^{+2.6}$	32.7	$0.71_{-0.31}^{+0.43} \pm 0.08$
10.8690	21.74	325_{-19}^{+20}	37.4	$1.61 \pm 0.10 \pm 0.12$	186 ± 15	18.9	$2.35 \pm 0.19 \pm 0.32$	$10.5_{-3.3}^{+4.0}$	1.5	$1.44_{-0.45}^{+0.55} \pm 0.19$

the coil is instrumented to detect K_L^0 mesons and to identify muons (KLM). The detector is described in detail elsewhere [13].

Events with four well-reconstructed charged tracks and zero net charge are selected to examine $\Upsilon(nS)\pi^+\pi^-$ production. A final state that is consistent with a $\Upsilon(nS)$ candidate and two charged pions is reconstructed. A $\Upsilon(nS)$ candidate is formed from two muons with opposite charges, where the muon candidates are required to have associated hits in the KLM detector that agree with the extrapolated trajectory of a charged track provided by the drift chamber. The other two charged tracks must have a low likelihood of being electrons; they are then treated as pion candidates. This suppresses the background, $e^+e^- \rightarrow \mu^+\mu^-\gamma \rightarrow \mu^+\mu^-e^+e^-$ with a photon conversion. (Electron identification is based on associating the ECL shower energy to the track momentum, dE/dx from CDC, and the ACC response.) The cosine of the opening angle between the π^+ and π^- momenta in the laboratory frame is required to be less than 0.95. The four-track invariant mass must satisfy $|M(\mu^+\mu^-\pi^+\pi^-) - \sqrt{s}| < 150 \text{ MeV}/c^2$. The trigger efficiency for four-track events satisfying these criteria is very close to 100%.

The kinematic variable ΔM , defined by the difference between $M(\mu^+\mu^-\pi^+\pi^-)$ and $M(\mu^+\mu^-)$, is used to identify the signal candidates. Sharp signal peaks are expected at $\Delta M = \sqrt{s} - M_{\Upsilon(nS)}$. The candidate events are separated into three distinct regions defined by $|\Delta M - [\sqrt{s} - M_{\Upsilon(nS)}]| < 150 \text{ MeV}/c^2$ for $n = 1, 2$, and 3, and signal yields are extracted by an unbinned extended maximum likelihood (ML) fit to the ΔM distribution within each region. The likelihood function for each fit is defined as

$$L(N_s, N_b) = \frac{e^{-(N_s+N_b)}}{N!} \prod_{i=1}^N [N_s \cdot P_s(\Delta M_i) + N_b \cdot P_b(\Delta M_i)], \quad (1)$$

where N_s (N_b) denotes the yield for signal (background), and P_s (P_b) is the signal (background) probability density function (PDF). The signal is modeled by a sum of two Gaussians while the background is approximated by a linear function. The Gaussians parameterized for the signal PDF are fixed from the Monte Carlo (MC) simulation at each energy point. We fit 18 ΔM distributions (shown in Fig. 1 with the fit results superimposed) simultaneously with common corrections on the mean and width of signal Gaussians.

The measured signal yields, reconstruction efficiencies, integrated luminosity, and the production cross sections, as well as the results from the previous publication [7] for the data sample collected at $\sqrt{s} = 10.869 \text{ GeV}$, are summarized in Table I. The efficiencies for $\Upsilon(3S)\pi^+\pi^-$ are much improved compared to Ref. [7] since the inefficient selection criterion $\theta_{\text{max}} < 175^\circ$ is removed, where θ_{max} is the maximum opening angle between any pair of charged tracks in the CM frame.

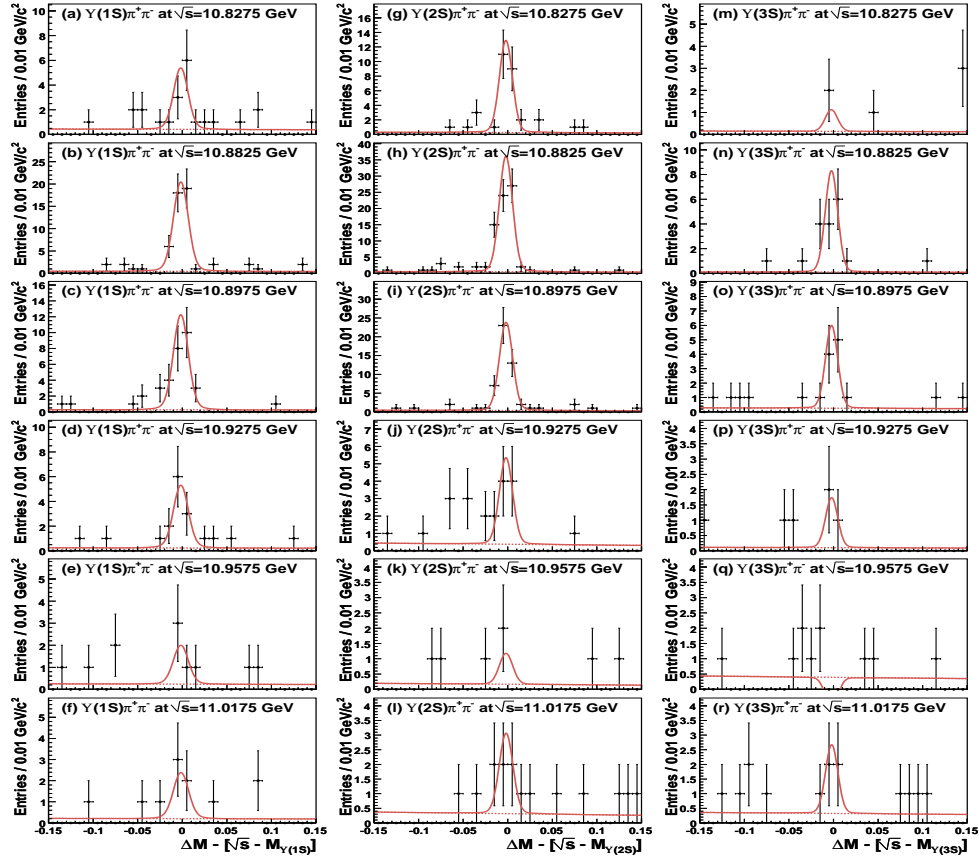


Figure 1: The distributions of $\Delta M - [\sqrt{s} - M_{\Upsilon(nS)}]$ ($n = 1, 2, 3$) for (a–f) $\Upsilon(1S)\pi^+\pi^-$, (g–l) $\Upsilon(2S)\pi^+\pi^-$, and (m–r) $\Upsilon(3S)\pi^+\pi^-$ events with the fit results superimposed. The different rows of plots represent the data samples collected at different CM energies. The dashed curves show the background components in the fits.

3. SYSTEMATIC UNCERTAINTIES

For the cross section measurements, systematic uncertainties are dominated by the $\Upsilon(nS) \rightarrow \mu^+\mu^-$ branching fractions, reconstruction efficiencies, and PDF parameterization for the fits. Uncertainties of 2.0%, 8.8%, and 9.6% for the $\Upsilon(1S)$, $\Upsilon(2S)$, and $\Upsilon(3S) \rightarrow \mu^+\mu^-$ branching fractions are included, respectively. For the $\Upsilon(1S)\pi^+\pi^-$ and $\Upsilon(2S)\pi^+\pi^-$ modes, the reconstruction efficiencies are obtained from MC simulations using the observed $M(\pi^+\pi^-)$ and $\cos\theta_{\text{Hel}}$ distributions in our previous publication as inputs. The uncertainties associated with these distributions give rise to 2.7%–4.5% and 1.9%–4.2% errors for the $\Upsilon(1S)\pi^+\pi^-$ and $\Upsilon(2S)\pi^+\pi^-$ efficiencies, respectively. The ranges on the uncertainty arise from the CM energy dependence. We use the model of Ref. [15] as well as a phase space model as inputs for $\Upsilon(3S)\pi^+\pi^-$ measurements; the differences in acceptance are included as systematic uncertainties. The uncertainties from PDF parameterization are estimated either by replacing the signal PDF with a sum of three Gaussians, or by replacing the background PDF with a second-order polynomial. The differences between these alternative fits and the nominal results are taken as the systematic uncertainties. Other uncertainties include: tracking efficiency (1% per charged track), muon identification (0.5% per muon candidate), electron rejection for the charged pions (0.1–0.2% per pion), trigger efficiencies (0.1–5.2%), and integrated luminosity (2.1%). The uncertainties from all sources are added in quadrature. The total systematic uncertainties are 7%–11%, 11%–16%, and 12%–14% for the $\Upsilon(1S)\pi^+\pi^-$, $\Upsilon(2S)\pi^+\pi^-$, and $\Upsilon(3S)\pi^+\pi^-$ channels, respectively.

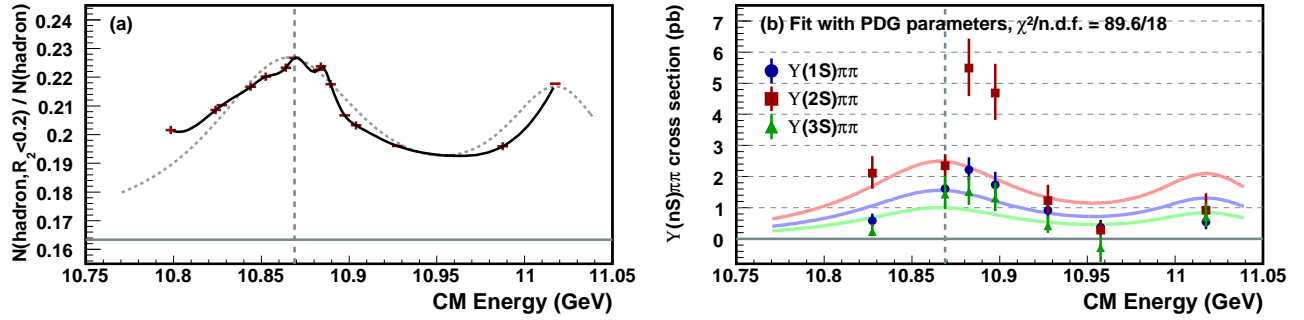


Figure 2: (a) The fraction of hadronic events with $R_2 < 0.2$ as a function of CM energy; (b) the energy dependent cross sections for $e^+e^- \rightarrow \Upsilon(nS)\pi^+\pi^-$ events, the result of a fit with the PDG $\Upsilon(10860)$ and $\Upsilon(11020)$ parameters is superimposed. The solid smooth curve in (a) is an interpolation of the $R_2 < 0.2$ fractions with a natural spline; the dashed smooth curve shows the summed Breit-Wigner resonant shapes for the $\Upsilon(10860)$ and $\Upsilon(11020)$; the horizontal line represents the fraction measured from an off-resonance sample (recorded at $\sqrt{s} \sim 10.52$ GeV). The vertical dashed line indicates the energy at which the hadronic cross section is maximal.

4. INTERPRETATIONS AND CONCLUSION

The resonance parameters for the $\Upsilon(10860)$ are examined using the energy scan data collected at the CM energies between 10.80 and 11.02 GeV. The results include the samples corresponding to an integrated luminosity of $\simeq 30$ pb $^{-1}$ at nine values of CM energy, and the samples of $\simeq 1$ fb $^{-1}$ at six CM energies, and the data sets collected near the peak of $\Upsilon(10860)$. The fraction of hadronic events with $R_2 < 0.2$ is shown as a function of CM energy in Fig. 2 (a), where R_2 is the ratio of the second to zeroth Fox-Wolfram moments [16]. The summed world average resonance shapes for $\Upsilon(10860)$ and $\Upsilon(11020)$ [17] are shown by the dashed curve, and are consistent with our measurements. A fit to the measured $\Upsilon(nS)\pi^+\pi^-$ cross sections using the PDG resonance parameters for the $\Upsilon(10860)$ and the $\Upsilon(11020)$, shown in Fig. 2 (b), has a quality of $\chi^2 = 89.6$ for 18 degrees of freedom, which is much worse than fits with the Breit-Wigner resonant shapes. An alternative fit using a natural spline interpolation of the hadronic fractions (also shown in Fig. 2 (a)) instead of the sum of two Breit-Wigner line shapes has a similar poor quality, $\chi^2 = 96.9$ for 18 degrees of freedom.

In summary, we report the observation of an enhancement in $e^+e^- \rightarrow \Upsilon(1S)\pi^+\pi^-$, $\Upsilon(2S)\pi^+\pi^-$, and $\Upsilon(3S)\pi^+\pi^-$ production based on a data sample collected at CM energies between $\sqrt{s} \simeq 10.83$ and 11.02 GeV. The energy-dependent cross sections for $e^+e^- \rightarrow \Upsilon(nS)\pi^+\pi^-$ events are measured for the first time, and the resonance structures are extracted by fits to the cross sections. A fit with a simple Breit-Wigner parameterization yields a mean value of $10889.6 \pm 1.8 \pm 1.5$ MeV/ c^2 and a width of $54.7^{+8.5}_{-7.2} \pm 2.5$ MeV/ c^2 , where the first uncertainty is statistical and the second is systematic. A second fit with separate shape parameters for $e^+e^- \rightarrow \Upsilon(1S)\pi^+\pi^-$, $\Upsilon(2S)\pi^+\pi^-$, and $\Upsilon(3S)\pi^+\pi^-$ final states is consistent with the fit with common mean and width within the statistical uncertainties. The observed cross section curve obtained from the fractions of hadronic events with $R_2 < 0.2$ is consistent with the previously measured shapes for the $\Upsilon(10860)$ and $\Upsilon(11020)$. However, a fit to the $e^+e^- \rightarrow \Upsilon(nS)\pi^+\pi^-$ cross sections with this hadronic curve has a poor χ^2 , indicating that the observed resonance structure disagrees with the known Υ states.

Acknowledgments

We thank the KEKB group for excellent operation of the accelerator, the KEK cryogenics group for efficient solenoid operations, and the KEK computer group and the NII for valuable computing and SINET3 network support. We acknowledge support from MEXT and JSPS (Japan); ARC and DEST (Australia); NSFC (China); DST

(India); MOEHRD, KOSEF and KRF (Korea); KBN (Poland); MES and RFAAE (Russia); ARRS (Slovenia); SNSF (Switzerland); NSC and MOE (Taiwan); and DOE (USA).

References

- [1] S. K. Choi *et al.* [Belle Collaboration], Phys. Rev. Lett. **91**, 262001 (2003).
- [2] B. Aubert *et al.* [BABAR Collaboration], Phys. Rev. Lett. **95**, 142001 (2005).
- [3] T. E. Coan *et al.* [CLEO Collaboration], Phys. Rev. Lett. **96** (2006) 162003.
- [4] C. Z. Yuan *et al.* [Belle Collaboration], Phys. Rev. Lett. **99**, 182004 (2007).
- [5] B. Aubert *et al.* [BABAR Collaboration], Phys. Rev. Lett. **98**, 212001 (2007).
- [6] X. L. Wang *et al.* [Belle Collaboration], Phys. Rev. Lett. **99**, 142002 (2007).
- [7] K. F. Chen *et al.* [Belle Collaboration], Phys. Rev. Lett. **100**, 112001 (2008).
- [8] W. S. Hou, Phys. Rev. D **74**, 017504 (2006).
- [9] Yu. A. Simonov, JETP Lett. **87**, 147 (2008).
- [10] C. Meng and K. T. Chao, Phys. Rev. D **77**, 074003 (2008); C. Meng and K. T. Chao, arXiv:0805.0143 [hep-ph].
- [11] M. Karliner and H. J. Lipkin, arXiv:0802.0649 [hep-ph].
- [12] S. Kurokawa and E. Kikutani, Nucl. Instrum. Methods Phys. Res., Sect. A **499**, 1 (2003), and other papers included in this Volume.
- [13] A. Abashian *et al.* [Belle Collaboration], Nucl. Instrum. Methods Phys. Res., Sect. A **479**, 117 (2002).
- [14] The helicity angle θ_{Hel} is the angle between the π^- and $\Upsilon(nS)\pi^+\pi^-$ momenta in the $\pi^+\pi^-$ rest frame.
- [15] L. S. Brown and R. N. Cahn, Phys. Rev. Lett. **35**, 1 (1975); M. B. Voloshin, JETP Lett. **21**, 347 (1975); Y. P. Kuang and T. M. Yan, Phys. Rev. D **24**, 2874 (1981).
- [16] G. C. Fox and S. Wolfram, Phys. Rev. Lett. **41**, 1581 (1978).
- [17] W.-M. Yao *et al.*, J. Phys. G **33**, 1 (2006).

